Hindawi
Advances in Mathematical Physics
Volume 2018, Article ID 5686089, 8 pages
https://doi.org/10.1155/2018/5686089

Research Article

Heat Transfer in MHD Flow due to a Linearly Stretching Sheet with Induced Magnetic Field

Tarek M. A. El-Mistikawy

Department of Engineering Mathematics and Physics, Faculty of Engineering, Cairo University, Giza 12211, Egypt

Correspondence should be addressed to Tarek M. A. El-Mistikawy; elmistikawy@eng.cu.edu.eg

Received 4 November 2017; Accepted 28 January 2018; Published 25 February 2018

Academic Editor: Alkesh Punjabi

The traditionally ignored physical processes of viscous dissipation, Joule heating, streamwise heat diffusion, and work shear are assessed and their importance is established. The study is performed for the MHD flow due to a linearly stretching sheet with induced magnetic field. Cases of prescribed surface temperature, heat flux, surface feed (injection or suction), velocity slip, and thermal slip are considered. Sample numerical solutions are obtained for the chosen combinations of the flow parameters.

1. Introduction

The problem of the two-dimensional flow due to a linearly stretching sheet, first formulated by Crane [1], has a simple exact similarity solution. This invited several researchers to add to it new features allowing for self-similarity. As a boundary-layer problem, Pavlov [2] added uniform transverse magnetic field. P. S. Gupta and A. S. Gupta [3] added surface feed (suction or injection). These problems were recognized as being exact solutions of the corresponding Navier-Stokes problems by Crane [1], Andersson [4], and Wang [5], respectively. To the Navier-Stokes problem, Andersson [6] added velocity slip. Fang et al. [7] combined the effects of transverse magnetic field, surface feed, and velocity slip.

Heat transfer was treated in several publications, mostly neglecting viscous dissipation and Joule heating (in MHD problems). This allowed self-similar formulation in cases of the surface having constant temperature [3, 8] or temperature or heat flux proportional to a power of the stretch-wise coordinate x [9–11]. Prasad and Vajravelu [12] treated the boundary-layer flow of a power law fluid retaining viscous dissipation and Joule heating, in case of the surface temperature being proportional to x^2.

The abovementioned MHD problems adopted the small magnetic Reynolds number assumption, thus neglecting the induced magnetic field. In [13], it was shown that the full MHD problem, that is, Navier-Stokes and Maxwell's equations with adherence conditions and appropriate magnetic conditions, allowed for self-similarity.

In this article, the work of [13] is extended to the heat transfer problem including viscous dissipation and Joule heating, in cases of prescribed surface temperature or heat flux. Surface feed, velocity and thermal slip, and shear work are also included.

The problem is of both theoretical and practical value. Theoretically, it indicates the importance of the traditionally ignored physical processes of induced magnetic field, viscous dissipation, Joule heating, and shear work. Practically, the problem is encountered in several situations. For example, extrusion processes in polymer and glass industries involve stretching sheets extruded in an otherwise quiescent fluid. The quality of the product depends on the controlled heat transfer between the sheet and the fluid. Four control agents are in mind, in this study, the MHD effect of a magnetic field permeating a conducting fluid, surface feed (fluid injection or suction), fluid additives (possibly, nanoparticles) associated with velocity and thermal slip [14], and convective heating or cooling [15] which has the same effect as thermal slip.

2. Mathematical Model

An electrically conducting, incompressible, and Newtonian fluid is driven by a nonconducting porous sheet, which is

stretching linearly in the x-direction. At the surface, we consider cases of prescribed temperature or heat flux and allow for velocity and thermal slip. In the far field, the fluid is essentially quiescent under pressure p_∞ and temperature T_∞ and is permeated by a stationary magnetic field of uniform strength B in the transverse y-direction.

The equations governing this steady MHD incompressible flow are the continuity and Navier-Stokes equations with Lorentz force [16]

$$\nabla \cdot V = 0 \tag{1}$$

$$\rho V \cdot \nabla V + \nabla p = \rho \nu \nabla^2 V + J \times B, \tag{2}$$

the energy equation with viscous dissipation and Joule heating

$$\rho c V \cdot \nabla T = k \nabla^2 T + \Phi + \sigma^{-1} J^2, \tag{3}$$

and Maxwell's equations and Ohm's law, in the absence of surplus charge and electric field,

$$\nabla \times B = \mu J \tag{4}$$

$$\nabla \cdot B = 0 \tag{5}$$

$$J = \sigma V \times B. \tag{6}$$

V is the velocity vector, p is the pressure, T is the temperature, J is the current density, B is the magnetic field, and Φ is the dissipation function. Constants are the fluid density ρ, kinematic viscosity ν, specific heat c, thermal conductivity k, the electric conductivity σ, and magnetic permeability μ.

Use of Ohm's law (6) to eliminate J from (2) to (4) and casting in Cartesian components lead to the following equations for two-dimensional flow.

$$\begin{aligned}
&u_x + v_y = 0,\\
&\rho\left(uu_x + vu_y\right) + p_x\\
&\quad = \rho\nu\left(u_{xx} + u_{yy}\right) + \sigma\left[(B+s)\, rv - (B+s)^2 u\right],\\
&\rho\left(uv_x + vv_y\right) + p_y\\
&\quad = \rho\nu\left(v_{xx} + v_{yy}\right) + \sigma\left[(B+s)\, ru - r^2 v\right],\\
&s_x - r_y = \sigma\mu\left[(B+s)\, u - rv\right],\\
&r_x + s_y = 0,\\
&\rho c\left(uT_x + vT_y\right)\\
&\quad = k\left(T_{xx} + T_{yy}\right) + \rho\nu\left[2\left({u_x}^2 + {v_y}^2\right) + \left(u_y + v_x\right)^2\right]\\
&\qquad + \sigma\left[(B+s)\, u - rv\right]^2.
\end{aligned} \tag{7}$$

They are complemented with the surface conditions

$$\begin{aligned}
y = 0: \quad & u = \omega x + \lambda_w u_y,\\
& v = v_w,\\
& T = T_w + \gamma_w T_y,\\
& \text{or } q_w = -kT_y - \rho\nu\lambda_w {u_y}^2,
\end{aligned} \tag{8}$$

and the far field conditions

$$\begin{aligned}
y \sim \infty: \quad & u \sim 0,\\
& p \sim p_\infty,\\
& r \sim 0,\\
& s \sim 0,\\
& T \sim T_\infty.
\end{aligned} \tag{9}$$

(u, v) are the velocity components in the (x, y) directions, respectively, and (r, s) are the corresponding induced magnetic field components. The stretching rate ω and the velocity and thermal slip coefficients λ_w and γ_w are assumed constant. In the condition for q_w, the last term represents the shear work [17]. In the far field, the condition for r translates the physical requirement of the absence of any current density, while that on s indicates that B stands for the far field total magnetic field imposed and induced [13].

The problem admits the similarity transformations

$$\begin{aligned}
&y = \sqrt{\frac{\nu}{\omega}}\eta,\\
&v = -\sqrt{\nu\omega}\, f(\eta),\\
&u = \omega x f',\\
&s = B\sigma\mu\nu g(\eta),\\
&r = -B\sigma\mu\sqrt{\nu\omega}\, x g',\\
&p = p_\infty - \rho\omega\nu\left[f' + \frac{1}{2}f^2 - \frac{1}{2}f^2(\infty)\right]\\
&\qquad - \frac{1}{2}B^2\sigma^2\mu\nu\omega x^2 g'^2,\\
&T = T_\infty + \frac{\nu\omega}{c}\left[\theta_0(\eta) + \sqrt{\frac{\omega}{\nu}}x\theta_1(\eta) + \frac{\omega}{\nu}x^2\theta_2(\eta)\right],
\end{aligned} \tag{10}$$

where primes denote differentiation with respect to η. The fact that the temperature is quadratic in x allows its constituents θ_0, θ_1, and θ_2 to be dependent on η only.

The problem becomes

$$\begin{aligned}
&f''' + ff'' - f'^2 - \beta f'\\
&\quad = -P_m\beta\left[g'^2 + (1 + P_m g)\, fg' - (2 + P_m g)\, f'g\right]
\end{aligned} \tag{11}$$

$$g'' = f' + P_m\left(gf' - fg'\right) \tag{12}$$

$$\begin{aligned}
&\mathrm{Pr}^{-1}\theta_2'' + f\theta_2' - 2f'\theta_2\\
&\quad = -\beta\left[f' + P_m\left(gf' - g'f\right)\right]^2 - f''^2
\end{aligned} \tag{13}$$

$$\mathrm{Pr}^{-1}\theta_1'' + f\theta_1' - f'\theta_1 = 0 \tag{14}$$

$$\mathrm{Pr}^{-1}\theta_0'' + f\theta_0' = -\mathrm{Pr}^{-1}2\theta_2 - 4f'^2, \tag{15}$$

where $P_m = \sigma\mu\nu$ is the magnetic Prandtl number, $\beta = \sigma B^2/\rho\omega$ is the magnetic interaction number, and $\Pr = \rho\nu c/k$ is the Prandtl number.

Consistent with the similarity transformations, we take the surface values to be

$$v_w = -\sqrt{\nu\omega} f_w,$$
$$T_w = T_\infty + \frac{\nu\omega}{c}\left[\Theta_0 + \sqrt{\frac{\omega}{\nu}}\Theta_1 x + \frac{\omega}{\nu}\Theta_2 x^2\right], \quad (16)$$
$$q_w = \frac{k\omega\sqrt{\nu\omega}}{c}\left[Q_0 + \sqrt{\frac{\omega}{\nu}}Q_1 x + \frac{\omega}{\nu}Q_2 x^2\right],$$

where f_w, Θ_0, Θ_1, Θ_2, Q_0, Q_1, and Q_2 are prescribed values.

With $\lambda = \lambda_w\sqrt{\omega/\nu}$ and $\gamma = \gamma_w\sqrt{\omega/\nu}$, we get the following conditions on the flow variables:

$$f(0) = f_w,$$
$$f'(0) = 1 + \lambda f''(0), \quad (17)$$
$$f'(\infty) = 0$$
$$g(\infty) = 0, \quad (18)$$
$$g'(\infty) = 0$$
$$\theta_2(0) = \Theta_2 + \gamma\theta_2'(0)$$
$$\text{or } \theta_2'(0) = -Q_2 - \Pr\lambda\left[f''(0)\right]^2, \quad (19)$$
$$\theta_2(\infty) = 0$$
$$\theta_1(0) = \Theta_1 + \gamma\theta_1'(0)$$
$$\text{or } \theta_1'(0) = -Q_1, \quad (20)$$
$$\theta_1(\infty) = 0$$
$$\theta_0(0) = \Theta_0 + \gamma\theta_0'(0)$$
$$\text{or } \theta_0'(0) = -Q_0, \quad (21)$$
$$\theta_0(\infty) = 0.$$

3. Numerical Method

We start by solving for $f(\eta)$ and $g(\eta)$, since their nonlinear problem is uncoupled from the problems for $\theta_2(\eta)$, $\theta_1(\eta)$, and $\theta_0(\eta)$. A closed form solution is not possible, so we seek an iterative numerical solution. In the nth iteration, we solve, for $f_n(\eta)$, (11) with its right hand side evaluated using the previous iteration solutions $f_{n-1}(\eta)$ and $g_{n-1}(\eta)$, together with conditions (17). Then we solve, for $g_n(\eta)$, (12) with the known $f_n(\eta)$, together with conditions (18). The iterations continue until the maximum error in $f(\eta_\infty)$, $f''(0)$, $g(0)$, and $g'(0)$ becomes less than 10^{-10}. For the first iteration, we zero the right hand side of (11) which corresponds to $g_0(\eta) = 0$.

The numerical solution of the problem for $f_n(\eta)$ and $g_n(\eta)$ utilizes Keller's two-point, second-order accurate, finite-difference scheme [18]. A uniform step size $\Delta\eta = 0.01$ is used on a finite domain $0 \le \eta \le \eta_\infty$. The value of $\eta_\infty = 60$ is chosen sufficiently large in order to insure the asymptotic satisfaction of the far field conditions. The nonlinear terms in the problem for $f_n(\eta)$ are quasi-linearized, and an iterative procedure is implemented, terminating when the maximum error in $f_n(\eta_\infty)$ and $f_n''(0)$ becomes less than 10^{-10}.

Having determined $f(\eta)$ and $g(\eta)$, we solve the linear problems: (13) with conditions (19) for $\theta_2(\eta)$, (14) with conditions (20) for $\theta_1(\eta)$, and then (15) with conditions (21) for $\theta_0(\eta)$, using Keller's scheme on the same grid.

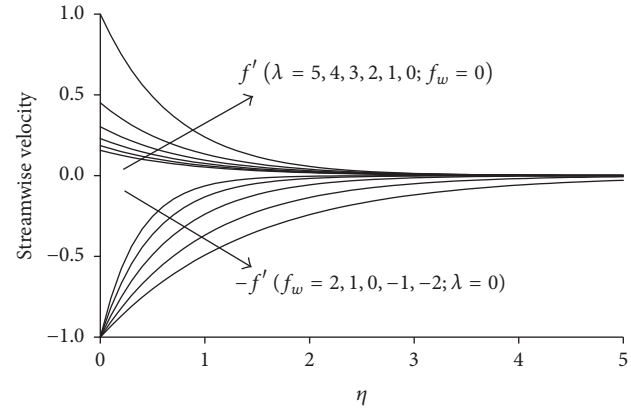

Figure 1: Streamwise velocity profile.

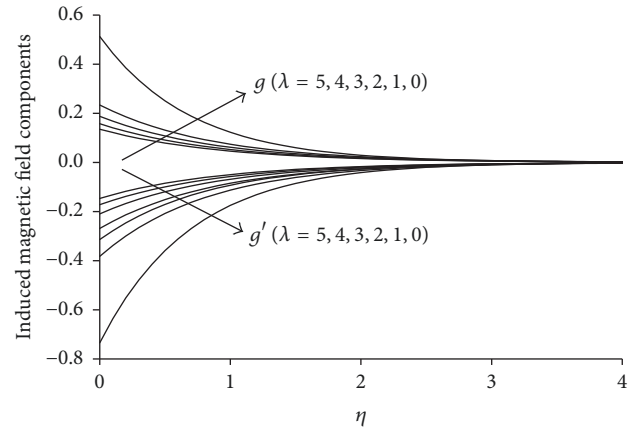

Figure 2: Profiles of induced magnetic field components; $f_w = 0$.

4. Sample Results and Discussion

The problem for $f(\eta)$ and $g(\eta)$ involves four parameters: P_m, β, λ, and f_w. For $P_m = 0.1$, $\beta = 1$, Figure 1 depicts $f'(\eta)$ at different values of λ, when $f_w = 0$, and at different values of f_w, when $\lambda = 0$. The corresponding results for $g(\eta)$ together with $g'(\eta)$ are depicted in Figures 2 and 3, respectively. The induced magnetic field is primarily affected by the streamwise velocity component represented by $f'(\eta)$. As $f'(\eta)$ decreases due to higher surface slip or suction rate, both $g(\eta)$ and $-g'(\eta)$ decrease.

Tables 1 and 2 give values of the surface shear and the entrainment rate represented, respectively, by $f''(0)$ and

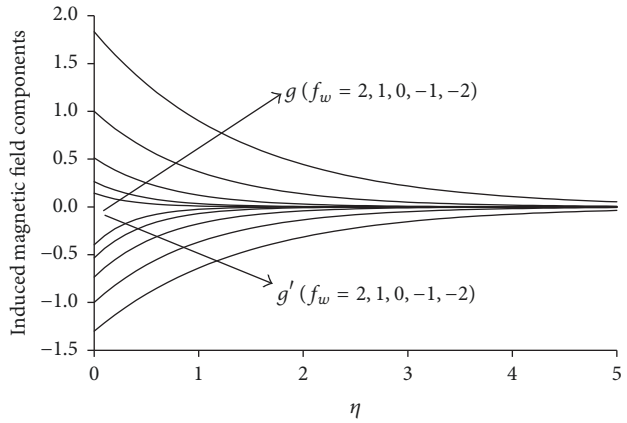

Figure 3: Profiles of induced magnetic field components; $\lambda = 0$.

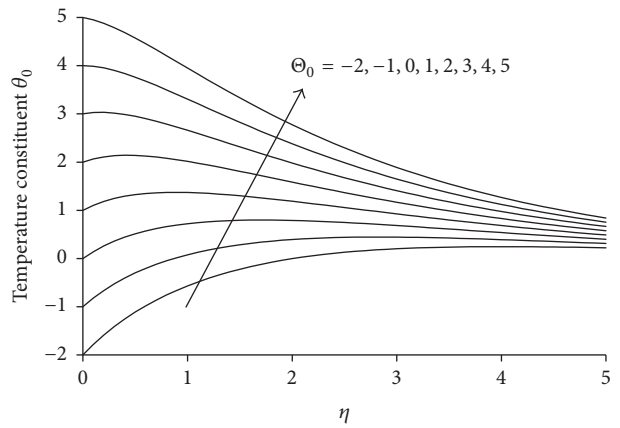

Figure 4: Temperature constituent $\theta_0(\eta)$ at different values of Θ_0.

Table 1: Variation of $f''(0)$, $f(\eta_\infty)$, $g(0)$, and $g'(0)$ with λ; $f_w = 0$.

λ	$f''(0)$	$f(\eta_\infty)$	$g(0)$	$g'(0)$
0	−1.43222	0.69822	0.51249	−0.73400
1	−0.54904	0.37039	0.31377	−0.38201
2	−0.34863	0.26290	0.23363	−0.26904
3	−0.25674	0.20564	0.18749	−0.20949
4	−0.20357	0.16944	0.15701	−0.17210
5	−0.16879	0.14431	0.13524	−0.14626

Table 2: Variation of $f''(0)$, $f(\eta_\infty)$, $g(0)$, and $g'(0)$ with f_w; $\lambda = 0$.

f_w	$f''(0)$	$f(\eta_\infty)$	$g(0)$	$g'(0)$
−2	−0.70972	−0.59099	1.83271	−1.30070
−1	−1.00000	0.00000	1.00000	−1.00000
0	−1.43222	0.69822	0.51249	−0.73400
1	−2.02629	1.49351	0.26293	−0.53278
2	−2.75888	2.36247	0.14369	−0.39641

$f(\infty)$, as well as the induced magnetic field components at the surface represented, respectively, by $g'(0)$ and $g(0)$. Refer to [13] for values of $f''(0)$, $f(\infty)$, $g'(0)$, and $g(0)$ at different values of P_m and β, when $\lambda = f_w = 0$.

Presented in Figures 4–9 are the results for the temperature constituents $\theta_0(\eta)$, $\theta_1(\eta)$, and $\theta_2(\eta)$ obtained, in case of prescribed surface temperature $T_w \propto x^a$, and in case of prescribed surface heat flux $q_w \propto x^a$; $a = 0, 1$ or 2. Table 3 summarizes the given surface values and the constituents involved in Figures 4–9, noting that (13)–(15) indicate that θ_1 and θ_2 are independent of the other constituents, while θ_0 depends on θ_2.

The following is noticed.

(i) *Constant surface temperature*: at $\Theta_0 = \Theta_{0c} \approx 4.04660$, $\theta_0'(0) = 0$. For $\Theta_0 > \Theta_{0c}$, $\theta_0'(0) < 0$ and θ_0 decreases monotonically with η, while for $\Theta_0 < \Theta_{0c}$, $\theta_0'(0) > 0$ and θ_0 has a peak that gets farther from the surface as Θ_0 decreases.

(ii) *Constant heat flux*: when $Q_0 = 0$, $\theta_0(0) \approx 8.39634$. As more heat is added to the fluid, that is, for increasing $Q_0 > 0$, $\theta_0(0)$ rises and θ_0 decreases monotonically with η. Removing more heat from the fluid, that is, for decreasing $Q_0 < 0$, $\theta_0(0)$ decreases and θ_0 has a peak that gets farther from the surface.

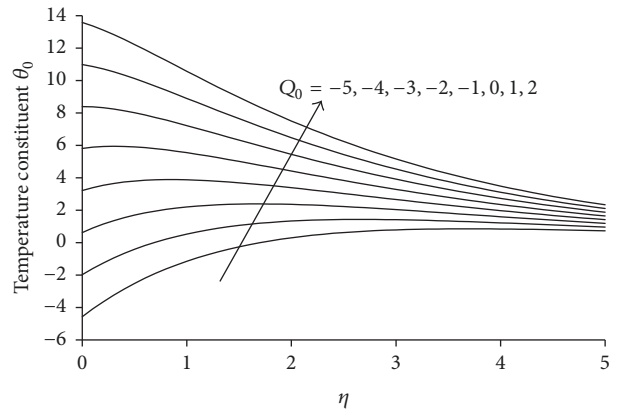

Figure 5: Temperature constituent $\theta_0(\eta)$ at different values of Q_0.

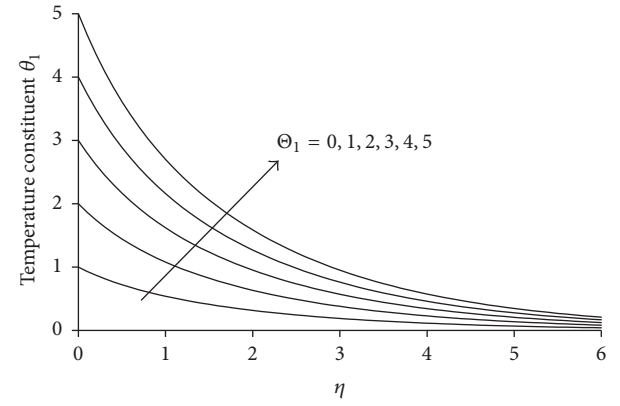

Figure 6: Temperature constituent $\theta_1(\eta)$ at different values of Θ_1.

(iii) *Linear surface temperature and heat flux*: noting that $\theta_1(-\Theta_1) = -\theta_1(\Theta_1)$ and $\theta_1(-Q_1) = -\theta_1(Q_1)$, the presented results for nonnegative Θ_1 and Q_1 indicate

Table 3: Data for Figures 4–9.

Case	Prescribed surface temperature			Prescribed surface heat flux		
Given	Θ_0 with $\Theta_1 = \Theta_2 = 0$	Θ_1 with $\Theta_0 = \Theta_2 = 0$	Θ_2 with $\Theta_0 = \Theta_1 = 0$	Q_0 with $Q_1 = Q_2 = 0$	Q_1 with $Q_0 = Q_2 = 0$	Q_2 with $Q_0 = Q_1 = 0$
Figure	Figure 4 for θ_0	Figure 6 for θ_1	Figure 8(a) for θ_2 Figure 8(b) for θ_0	Figure 5 for Q_0	Figure 7 for Q_1	Figure 9(a) for Q_2 Figure 9(b) for Q_0
Fixed parameters: Pr = 0.72, $P_m = 0.1$, $\beta = 1$, and $\lambda = f_w = \gamma = 0$						

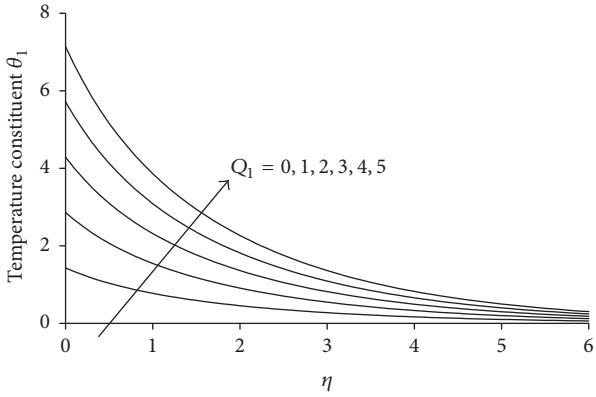

Figure 7: Temperature constituent $\theta_1(\eta)$ at different values of Q_1.

that θ_1 decreases monotonically with η. Higher Θ_1 results in smaller $\theta_1'(0) < 0$, while higher Q_1 results in higher $\theta_1(0)$.

(iv) *Surface temperature* $\propto x^2$: at $\Theta_2 = \Theta_{2c1} \approx 0.65967$, $\theta_2'(0) = 0$. For $\Theta_2 > \Theta_{2c1}$, $\theta_2'(0) < 0$ and θ_2 decreases monotonically with η. For $\Theta_{2c1} > \Theta_2 > \Theta_{2c2} \approx -0.33596$, $\theta_2'(0) > 0$ and θ_2 has a peak that gets farther from the surface as Θ_2 decreases. For $\Theta_2 < \Theta_{2c2}$, $\theta_2'(0) > 0$ and θ_2 rises monotonically with η. At $\Theta_2 = \Theta_{2c3} \approx -0.61370$, $\theta_0'(0) = 0$ and θ_0 drops from its zero surface value to a local minimum and then rises to its zero far field value. Similar behavior of θ_0 is observed for decreasing $\Theta_2 < \Theta_{2c3}$, but with decreasing minimum and $\theta_0'(0) < 0$. For increasing $\Theta_2 \geq \Theta_{2c4} \approx -0.33807$, $\theta_0'(0) > 0$ and θ_0 rises to a higher peak. For $\Theta_{2c3} < \Theta_2 < \Theta_{2c4}$, $\theta_0'(0) > 0$ and θ_0 rises to a peak, falls to zero and then to a bottom, and rises again to zero.

(v) *Heat flux* $\propto x^2$: when $Q_2 = 0$, $\theta_2(0) \approx 0.65967$. For increasing $Q_2 > 0$, $\theta_2(0)$ rises and θ_2 decreases monotonically with η. For decreasing $0 > Q_2 > Q_{2c1} \approx -0.96228$, $\theta_2(0)$ decreases from positive to negative values with θ_2 having a positive peak. For $Q_2 \leq Q_{2c1}$, θ_2 rises monotonically from a negative surface value to zero. For $Q_2 \geq Q_{2c2} \approx -0.98114$, θ_0 is monotonically decreasing, while for $Q_2 \leq Q_{2c3} \approx -1.96520$, θ_0 is monotonically increasing from its surface value to zero. For $Q_{2c3} < Q_2 < Q_{2c2}$, θ_0 decreases to a negative local minimum and then rises to zero.

To complement Figures 4–9, we give in Table 4 the numerical values of $\theta_0'(0)$ at different values of Θ_0, $\theta_1'(0)$ at different values of Θ_1, and $\theta_2'(0)$ and $\theta_0'(0)$ at different values of Θ_2, and in Table 5 the numerical values of $\theta_0(0)$ at different values of Q_0, $\theta_1(0)$ at different values of Q_1, and $\theta_2(0)$ and $\theta_0(0)$ at different values of Q_2.

Table 6 shows the effect of the thermal slip coefficient γ. As the first legs of conditions (19)–(21) indicate, the sign of the surface derivative of the temperature constituent determines whether the surface value of the constituent increases or decreases with γ. Thus, for example, $\theta_2(0)$ increases when $\Theta_2 = 0$, for which $\theta_2'(0) > 0$, and decreases when $\Theta_2 = 1$, for which $\theta_2'(0) < 0$.

The shear work is represented by the term involving the velocity slip coefficient λ in the second leg of conditions (19) for $\theta_2'(0)$. Table 7 demonstrates its importance. Neglecting the shear work reduces the predicted surface temperature.

On the right-hand side of (13) and (15), the first terms represent Joule heating and streamwise heat diffusion, respectively, while the second terms represent heat dissipation. Table 8 demonstrates the effect of neglecting these three processes. The predicted heat flux to the surface, represented by $\theta_0'(0)$ and $\theta_2'(0)$, is reduced considerably by neglecting viscous dissipation, streamwise diffusion, and/or Joule heating. Neglecting one or more may even predict heat flux in the wrong direction.

5. Conclusion

The problem of the flow due to a linearly stretching sheet in the presence of a transverse magnetic field has been formulated to include surface feed, velocity slip, and thermal slip. The problem has been shown to admit self-similarity of the full MHD fluid flow equations. Included in the thermal equation and conditions are physical processes such as viscous dissipation, Joule heating, streamwise heat diffusion, and shear work which were traditionally ignored or approximated.

The presented numerical results are sample results. They show that the self-similar model (with the several physical processes involved) and the method of solution are capable of producing meaningful and useful results. No attempt is made to present a detailed study of the individual or collective effect

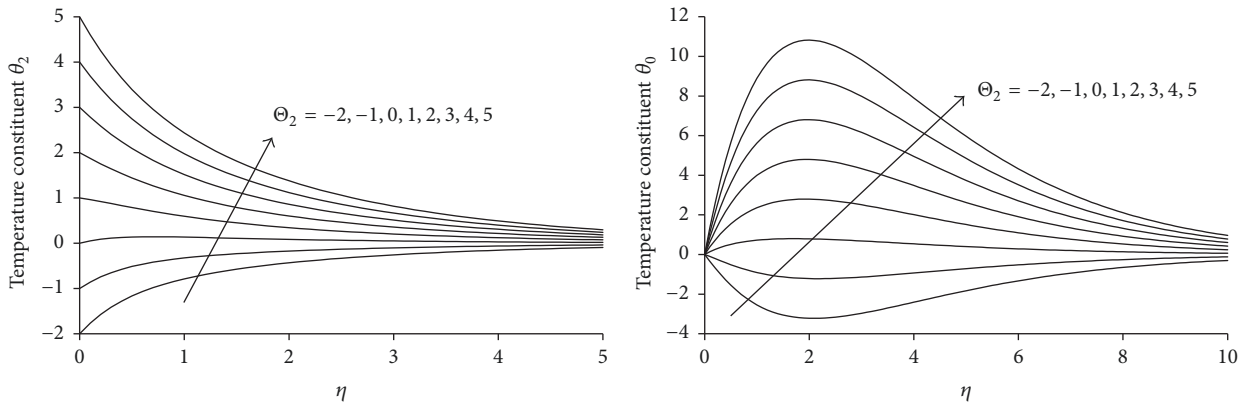

(a) Temperature constituent $\theta_2(\eta)$ at different values of Θ_2 (b) Temperature constituent $\theta_0(\eta)$ at different values of Θ_2

Figure 8

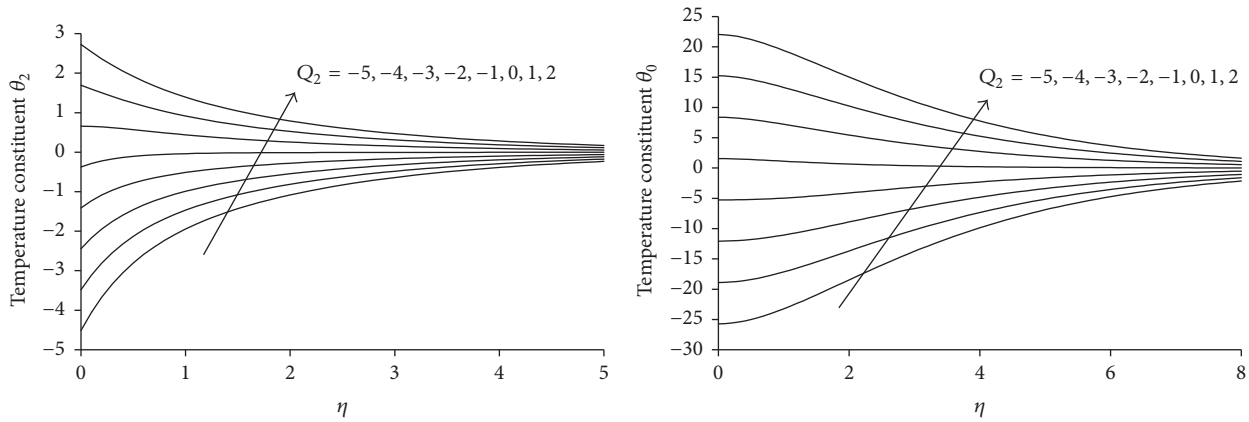

(a) Temperature constituent $\theta_2(\eta)$ at different values of Q_2 (b) Temperature constituent $\theta_0(\eta)$ at different values of Q_2

Figure 9

Table 4: Dependence of temperature gradients at surface on surface temperatures; $\gamma = 0$.

Θ_0	$\theta_0'(0)$	Θ_1	$\theta_1'(0)$	Θ_2	$\theta_2'(0)$	$\theta_0'(0)$
−2	2.33284	−2	1.39994	−2	2.57058	−3.52671
−1	1.94703	−1	0.69997	−1	1.60408	−0.98274
0	1.56122	0	0.00000	0	0.63757	1.56122
1	1.17541	1	−0.69997	1	−0.32893	4.10518
2	0.78960	2	−1.39994	2	−1.29543	6.64915
3	0.40379	3	−2.09991	3	−2.26194	9.19311
4	0.017978	4	−2.79988	4	−3.22844	11.73707
5	−0.36783	5	−3.49985	5	−4.19495	14.28104

Table 5: Dependence of temperatures at surface on surface heat fluxes; $\lambda = 0$.

Q_0	$\theta_0(0)$	Q_1	$\theta_1(0)$	Q_2	$\theta_2(0)$	$\theta_0(0)$
2	13.58023	2	2.85727	2	2.72898	22.04100
1	10.98828	1	1.42863	1	1.69433	15.21867
0	8.39634	0	0.00000	0	0.65967	8.39634
−1	5.80439	−1	−1.42863	−1	−0.37499	1.57401
−2	3.21245	−2	−2.85727	−2	−1.40964	−5.24832
−3	0.62051	−3	−4.28590	−3	−2.44430	−12.07065
−4	−1.97144	−4	−5.71454	−4	−3.47896	−18.89298
−5	−4.56338	−5	−7.14317	−5	−4.51361	−25.71531

Table 6: Effect of thermal slip coefficient γ; $\lambda = 0$.

γ	$\theta_0(0)$	$\theta_2(0)$	$\theta_0(0)$	$\theta_1(0)$	$\theta_2(0)$
0	0.00000	0.00000	1.00000	1.00000	1.00000
1	1.72175	0.32422	2.44335	0.58825	0.83273
2	3.01106	0.43476	3.57551	0.41668	0.77570
3	3.90609	0.49050	4.36960	0.32259	0.74695
4	4.55249	0.52410	4.94569	0.26317	0.72961
5	5.03861	0.54657	5.38001	0.22223	0.71802
Case	$\Theta_0 = \Theta_1 = \Theta_2 = 0$		$\Theta_0 = 1$ $\Theta_1 = \Theta_2 = 0$	$\Theta_1 = 1$ $\Theta_0 = \Theta_2 = 0$	$\Theta_2 = 1$ $\Theta_0 = \Theta_1 = 0$

Table 7: Effect of shear work; $Q_0 = Q_1 = Q_2 = 0$, $\gamma = 0$.

λ	$\theta_0(0)$	$\theta_2(0)$	$\theta_2'(0)$	$\theta_0(0)$	$\theta_2(0)$
0	8.39634	0.65967	0.00000	8.39634	0.65967
0.2	9.69402	0.66777	−0.16337	7.84848	0.47205
0.4	11.16024	0.65306	−0.21129	7.62154	0.36953
0.6	12.75638	0.63416	−0.22379	7.54814	0.30418
0.8	14.46870	0.61552	−0.22308	7.56234	0.25866
1	16.29111	0.59830	−0.21704	7.63203	0.22505
Case	Retaining shear work			Neglecting shear work	

Table 8: Neglect of viscous dissipation, streamwise diffusion, or Joule heating; $\Theta_1 = \Theta_2 = 0$.

Θ_0	$\theta_0'(0)$	$\theta_0'(0)$	$\theta_0'(0)$	$\theta_0'(0)$
0	0.22395	0.92158	1.33727	1.56122
1	−0.16186	0.53577	0.95146	1.17541
2	−0.54767	0.14996	0.56564	0.78960
3	−0.93348	−0.23585	0.17983	0.40379
4	−1.31929	−0.62166	−0.20598	0.017978
5	−1.70510	−1.00748	−0.59179	−0.36783
Case	Neglecting dissipation	Neglecting diffusion	Neglecting Joule heating	Retaining all
$\theta_2'(0)$	0.22323	0.63757	0.41434	0.63757

of the 12 parameters at hand. It is up to the interested reader to choose his/her set of processes and associated parameters to concentrate on. Moreover, other physical processes can be added to the model such as thermal radiation, heat generation, and/or flow through a porous medium, as long as self-similarity is preserved.

Nonetheless, the presented results pinpoint some interesting observations described below.

The velocity slip coefficient λ and the suction rate f_w have opposite effects on the curvature of the streamwise velocity profile $f'(\eta)$. While increasing the first flattens the profile causing the surface shear $|f''(0)|$ to decrease, increasing the second curls the profile causing $|f''(0)|$ to increase. The more the curling (flattening) of the $f'(\eta)$ profile, the higher (the lower) the far field entrainment rate $f(\infty)$, to compensate for the faster (the slower) streamwise flow close to the surface.

The induced magnetic field is primarily affected by the streamwise velocity component $f'(\eta)$. As $f'(\eta)$ decreases due to higher surface slip or suction rate, both $g(\eta)$ and $-g'(\eta)$ decrease.

The effect of the velocity slip coefficient λ and the suction rate f_w on the temperature is through their effect on the velocity and magnetic field components, with their involvement in viscous dissipation and Joule heating. Moreover, the velocity slip coefficient λ has the added effect of shear work, neglect of which results in considerable reduction in the predicted surface temperature.

Even when the surface is maintained at the ambient temperature T_∞, the fluid adjacent to the surface acquires a higher temperature that increases as the thermal slip coefficient γ increases. This is due to viscous dissipation and Joule heating, which are traditionally ignored. The same

applies to the equivalent situation of convective heating when the temperature on the other side of the sheet is maintained at T_∞, with γ being the heat convection coefficient.

The streamwise heat diffusion, which is neglected in boundary-layer models, is as important as viscous dissipation and Joule heating. Neglecting one or more of these thermal processes may predict lower heat flux or even heat flux in the wrong direction.

Depending on the surface thermal conditions, the profiles of the temperature constituents my decay monotonically toward the far field or may have an extremum at a finite distance from the surface. The critical condition corresponding to the extremum being at the surface separates cases of heat transfer to and from the surface.

Conflicts of Interest

The author declares that there are no conflicts of interest regarding the publication of this paper.

References

[1] L. J. Crane, "Flow past a stretching plate," *Zeitschrift für Angewandte Mathematik und Physik (ZAMP)*, vol. 21, no. 4, pp. 645–647, 1970.

[2] K. B. Pavlov, "Magnetohydrodynamic flow of an incompressible viscous fluid caused by deformation of a plane surface," *Magnetohydrodynamics* , vol. 10, no. 4, pp. 507–510, 1974.

[3] P. S. Gupta and A. S. Gupta, "Heat and mass transfer on a stretching sheet with suction and blowing," *The Canadian Journal of Chemical Engineering*, vol. 55, no. 6, pp. 744–746, 1977.

[4] H. I. Andersson, "An exact solution of the Navier-Stokes equations for magnetohydrodynamic flow," *Acta Mechanica*, vol. 113, no. 1-4, pp. 241–244, 1995.

[5] C. Y. Wang, "Analysis of viscous flow due to a stretching sheet with surface slip and suction," *Nonlinear Analysis: Real World Applications*, vol. 10, no. 1, pp. 375–380, 2009.

[6] H. I. Andersson, "Slip flow past a stretching surface," *Acta Mechanica*, vol. 158, no. 1-2, pp. 121–125, 2002.

[7] T. Fang, J. Zhang, and S. Yao, "Slip MHD viscous flow over a stretching sheet—an exact solution," *Communications in Nonlinear Science and Numerical Simulation*, vol. 14, no. 11, pp. 3731–3737, 2009.

[8] B. K. Dutta, P. Roy, and A. S. Gupta, "Temperature field in flow over a stretching sheet with uniform heat flux," *International Communications in Heat and Mass Transfer*, vol. 12, no. 1, pp. 89–94, 1985.

[9] L. J. Grubka and K. M. Bobba, "Heat transfer characteristics of a continuous stretching surface with variable temperature," *Journal of Heat Transfer*, vol. 107, no. 1, pp. 248–250, 1985.

[10] K. Vajravelu and D. Rollins, "Heat transfer in an electrically conducting fluid over a stretching surface," *International Journal of Non-Linear Mechanics*, vol. 27, no. 2, pp. 265–277, 1992.

[11] I.-C. Liu, "A note on heat and mass transfer for a hydromagnetic flow over a stretching sheet," *International Communications in Heat and Mass Transfer*, vol. 32, no. 8, pp. 1075–1084, 2005.

[12] K. V. Prasad and K. Vajravelu, "Heat transfer in the MHD flow of a power law fluid over a non-isothermal stretching sheet," *International Journal of Heat and Mass Transfer*, vol. 52, no. 21-22, pp. 4956–4965, 2009.

[13] T. M. El-Mistikawy, "MHD flow due to a linearly stretching sheet with induced magnetic field," *Acta Mechanica*, vol. 227, no. 10, pp. 3049–3053, 2016.

[14] D. Pal and G. Mandal, "Influence of Lorentz force and thermal radiation on heat transfer of nanofluids over a stretching sheet with velocity-thermal slip," *International Journal of Applied and Computational Mathematics*, vol. 3, no. 4, pp. 3001–3020, 2017.

[15] O. D. Makinde and A. Aziz, "Boundary layer flow of a nanofluid past a stretching sheet with a convective boundary condition," *International Journal of Thermal Sciences*, vol. 50, no. 7, pp. 1326–1332, 2011.

[16] G. W. Sutton and A. Sherman, *Engineering Magnetohydrodynamics*, McGraw-Hill, New York, NY, USA, 1965.

[17] C. Hong and Y. Asako, "Some considerations on thermal boundary condition of slip flow," *International Journal of Heat and Mass Transfer*, vol. 53, no. 15-16, pp. 3075–3079, 2010.

[18] H. B. Keller, "Accurate difference methods for linear ordinary differential systems subject to linear constraints," *SIAM Journal on Numerical Analysis*, vol. 6, pp. 8–30, 1969.